MODELLING WORKSTATION FOR A KRYPTON CONDENSER SYSTEM

Alexandre Moraux[1], Marco Pezzetti[2], Herve Coppier[2], Ahmed Rachid[3], Mohammed Chadli[3]

[1]European Organization for Nuclear Research, Physics Division
Geneva 23, Switzerland
[2]ESIEE Amiens, Laboratory of Energetics Needs Control
Amiens, France
[3]Picardie Jules Verne University, Faculty of Sciences and Health
Amiens, France

Alexandre.Moraux@cern.ch(Alexandre Moraux)

Abstract

This paper describes the design and the implementation of a Modelling WorkStation (MWS), which integrates a model of a cryogenics process. Its aim is to solve with adaptive control strategy non linearity and operating scenario's problems. This solution is developed at CERN on the NA48 experiment, started in the 90's. The slow control for the cryogenic detector is operated by Programmable Logic Controller (PLC). It will be changed in the current year, maintaining the liquid krypton thermal stability. The system components modeled are a krypton condenser based on an argon bath and a liquid nitrogen two phase heat exchanger. The First Principle model consists of mass and energy balances equations to represent the cryogenics dynamics of two phase flows. To face the limitations of the actual PI controller, a state space model with unknown terms, linked with a "cryogenic fluid library" to determine thermal coefficients, is developed to show the improvements possibilities in terms of thermal stability. In a second time, an extended model is presented, in order to optimize later, transient periods and to obtain prescribed behavior during the different operating ranges. It provides observation of the liquid nitrogen evaporation within the two phase heat exchanger resulting in a better efficiency for the use of cryogenic fluids. Model validation is based on measurements and on dynamic response analysis. The final part develops the model integration approach and the OPC communication between the MWS and the PLC to discharge the latter from the dynamic model and the controller coefficients calculation.

Keywords: Modelling, Cryogenics, TDC, Observation, PLC.

Presenting Author's Biography

Alexandre Moraux. Graduated by the engineering degree of the Graduate School of Electronic and Electrical Engineering of Amiens (ESIEE) and by the Master degree of the Technological University of Compiègne (UTC) in 2006, he is specialized in electrical systems and in Control Theory. He is currently doing his PhD at the LTI laboratory (Amiens) on cryogenic modelling and control, working as project associate at CERN in Geneva, Switzerland.

ISBN 978-3-901608-32-2

1 Introduction

The NA48 experiment was designed at CERN more than 10 years ago and aimed to measure the direct CP violation in the K^0-$\bar{K}^0$ system (Neutral Kaon and Antikaon). Part of the experiment is an electromagnetic calorimeter filled with 9000 liters of liquid krypton. For 10 years, the cryogenic system has operated under good conditions, controlled by Siemens S5 PLC. Recently, a new proposal in the use of the NA48 detectors, has implied to consider an upgrade needs of the cryogenics control system. Moreover, CERN faces technical support problems, due to the laboratory lack of expertise and changes on actual control algorithms are risky. Consequently, CERN plans to replace the cryogenics control system by a new one based on UNICOS/CERN standard in the current year.

2 Process Description

The purpose of the cryogenic system is to provide stable thermal conditions (120 K) in the liquid krypton when the calorimeter is in operation, and to ensure safe and loss-free storage of the liquid during long idle periods [1]. Direct cooling of the krypton with liquid nitrogen is only used in emergency cases because it makes the precise temperature control difficult due to the large temperature difference between the two liquids. To overcome this problem, a krypton condenser using liquid argon as intermediate coolant, has been installed. It forms a separate unit outside the cryostat to re-liquefy the gas evaporating from the calorimeter. The cold surface, around 3 m^2, is made of 230 vertical pipes, which tops are connected to the argon reservoir. The evaporated krypton gas (around $450\ l/min$ of gas under a static heat input of approximatively $3.3\ kW$, equivalent to $0.64\ l/min$ of liquid) is brought in thermal contact with the heat exchanger cooled from the bath of saturated liquid argon at 10 bars ($117\ K$), slightly above the triple point of krypton [2].

During data taking, the krypton pressure needs to be regulated to a value of (1.05 ± 0.01) bars. The argon is cooled by liquid nitrogen flowing through a heat exchanger in the gas space of the vessel. The nitrogen flow is controlled by the inlet valve such as to maintain the argon bath pressure constant to tend to a stable equilibrium point under a constant heat input. To compensate varying dynamic heat loads, the argon pressure needs to be part of the global approach in the modelling process. The outlet valve of the nitrogen heat exchanger regulates the inner pressure. A schematic of the krypton condenser is shown Fig. 1. In order to improve the efficiency of the cryogenic fluids and their control, this article proposed to integrate in the new control architecture, a parallel station exchanging data with the PLC, which objective is to estimate several parameters related to the liquid nitrogen heat exchanger and to optimize krypton condensation and nitrogen evaporation through a modelling approach of this component.

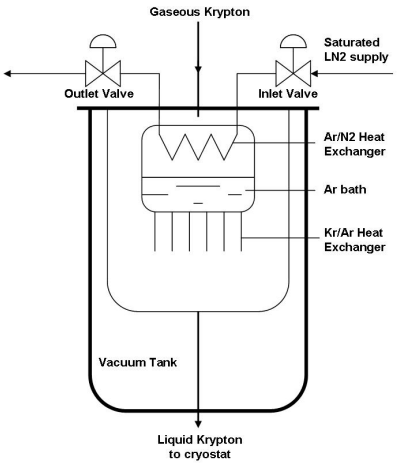

Fig. 1 The Liquid krypton condenser.

3 Dynamic krypton condenser model

Several condenser models have been estimated but most of them are not developed in a control perspective. The objective of this part is to obtain a low order model by basing our approach on ordinary differential equations (ODE), which represent the heat transfer between the cryogenic fluids. Due to the large variations of some thermal coefficients close to the saturation, it is sometimes necessary to take them into account, but not as a time derivative variable. Consequently, their values have to be determined with a "cryogenic fluid library" which contains the interesting parameters for krypton, argon and nitrogen. Considering the changes in argon and krypton as isochoric (constant density), vapor quality is directly related to saturated temperature. We do not include neither the pressure drop in the heat exchanger, nor the losses in the argon cooler, i.e. we consider the vacuum isolation as perfect.

3.1 Heat transfer coefficients estimation

One of the main problem is to find an approximation for the heat transfer coefficients between fluids. Several researches on this coefficient have been proposed for microfin tubes such as L. Dorretti and al. [3] and Kandlikar and Raykoff [4]. For the following determination, we will consider two heat transfer areas: 1) area between argon and krypton, 2) area between argon and nitrogen.

On the one hand of the first area, the "heating surface" is immerged in liquid argon. Regarding the phase change of argon, and the similarity with natural convection, "Pool boiling" phenomenon occurs. Several surveys for cryogenic applications on boiling heat transfer have been presented [5]. Pool boiling curve is given in [6] where the heat transfer coefficient is a function of temperature difference between the heating surface and the saturated temperature of the boiling liquid. High nonlinearities in this function can be reduced to 4 linear regions determining the boiling regime. On the other

ISBN 978-3-901608-32-2

hand, krypton condensation appears. The correlation of the condensation heat transfer coefficient was developed by Nusselt in 1916, as shown in [6], as a function of the Nusselt number, the length of the tubes and the liquid thermal conductivity. In the second area, the nitrogen mass flow and the evaporation process inside the heat exchanger tube induce a "forced convection boiling", and outside the heat exchanger, an argon condensation occurs. In our approach, the heat transfer coefficients between argon and krypton, and between argon and nitrogen, are defined as global exchange coefficients H_1, and H_2 as shown in Eq. (1), where L is the heat exchanger length, λ the thermal conductivity of the solid interface, R_i and R_e are respectively the internal and external radii, and h_i and h_e the internal and external heat transfer coefficients.

$$\frac{1}{H_2} = \frac{1}{2\pi \cdot L}\left[\frac{1}{h_i \cdot R_i} + \frac{\ln \frac{R_e}{R_i}}{\lambda} + \frac{1}{h_e \cdot R_e}\right] \quad (1)$$

Consequently, for the H_1 correlation, h_i represents the argon boiling heat transfer coefficient and h_e the krypton condensation heat transfer coefficient. h_i and h_e for H_1 and H_2 are determined from [6], [7], and [8]. If the exchange area has not the same surface on both side, typically in our case between argon and krypton, we report H to the "hot side", noted H_h, and to the "cold side", noted H_c.

3.2 Balances equations

Models for pressure vessels of different levels of complexity using thermal modelling approaches have been developed by S. Estrada-Flores [9]. Rigorous thermodynamic approach, where the transitions between states for liquid and vapor zones are detailed, is confronted with less complex models. In control engineering, modelling is used to improve the control system ability to follow the given set points. In two-phase fluids systems, the interactions between gas and liquid are causing non linear behavior and might easily bring the system outside the validity envelope of a linearized model. Low order models for two-phase fluids systems are not so implicit and require some assumptions. E. Skogestad and al. [10] observed the macro-scale behavior rather than the detailed physics that governs flow to easily use their model in a control perspective, such as G. Nygaard and G. Nævdal in [11] who focused on pressure and mass balances to design their model of two-phase flow for an oil well drilling.

The governing choice in our model equation must be the degree of precision we aim. We consider the exchanges between fluids following the newton empirical law with global heat transfer coefficient, which represents vaporization on one side, condensation on the other side, and thermal conduction of the interface. We assume that axial heat conduction in liquid nitrogen and heat conduction in argon between fluid layers are negligible and liquid and gas temperature for each fluid are the same. The two main variables in saturated fluids are temperature and quality. We can easily correlate them with their respective pressure. We will reduce our model to the temperatures control [T_{Kr}, T_{Ar}] using mass variation. In our first modelling approach, the manipulated variable is only nitrogen mass flow.
First, we consider "argon system" through vapor mass balance equation detailed in Eq. (2), where $M_{g,Ar}$ is argon vapor mass.

$$\frac{\mathrm{dM_{g,Ar}}}{\mathrm{dt}} = \frac{q_{1c}}{h_{lg,Ar}} - \frac{q_2}{h_{lg,Ar}} \quad (2)$$

$q_{1c}/h_{lg,Ar}$ represents the rate of liquid argon evaporating into vapor and $q_2/h_{lg,Ar}$ the rate of gaseous argon liquefying. $h_{lg,Ar} = h_{g,Ar} - h_{l,Ar}$ introduces h_l and h_g, respectively argon saturated liquid and vapor enthalpies. From Eq. (2), we can substitute argon vapor mass variations by respective volume and density. Argon vapor volume is much larger than liquid volume and considered as almost constant.

$$V_{Ar}\frac{d\rho_{g,Ar}\left(T_{Ar}\right)}{dT_{Ar}}\frac{dT_{Ar}}{dt} = \frac{q_{1c}}{h_{lg,Ar}} - \frac{q_2}{h_{lg,Ar}} \quad (3)$$

$\rho_{g,Ar}$ is the argon saturated vapor density in a function of the evaporating temperature T_Ar. According to small root mean squared error, curve fitting tools provide by regression a second order polynomial expression of density in a function of argon saturated temperature. We observe that first derivative vary from 2.04 to $3.86\ kg \cdot m^{-3} \cdot K^{-1}$ between $110\ K$ and $124\ K$, and cannot be assimilated to a constant. We introduce k_1 as described in Eq. (4).

$$k_1 = V_{Ar}\frac{d\rho_{Ar,g}\left(T_{Ar}\right)}{dT_{Ar}} \quad (4)$$

Assuming nitrogen temperature is constant between inlet and outlet valves, we describe the heat transferred from argon to nitrogen as the percentage of nitrogen mass flow evaporated along the heat exchanger tube. Nitrogen saturated pressure inside the heat exchanger is controlled by the outlet valve and modifies nitrogen latent heat of vaporization, as shown in Fig 2. As a result, nitrogen pressure can change argon condensation velocity, in extracting more or less heat, and so, system

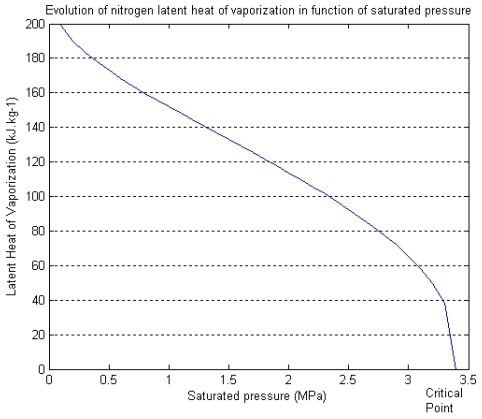

Fig. 2 Nitrogen latent heat of vaporization in a function of respective saturated pressure.

velocity. In our first model, we do not include nitrogen pressure control. Parallel studies and identification on pressure control inside heat exchanger have converged to first order model, well regulated by its own PI controller.

Based on the same development done previously for argon system, krypton saturated temperature variation is written in Eq. (5).

$$\frac{dT_{Kr}}{dt} = \frac{q}{k_2 \cdot h_{lg,Kr}} - \frac{q_{1h}}{k_2 \cdot h_{lg,Kr}} \tag{5}$$

q introduces heat inputs in the calorimeter we can divide into two terms: the static heat inputs q_s, which are approximately $3.3\,kW$, and the dynamic heat inputs q_d. $q/h_{lg,Kr}$ can be related to krypton vaporization per time unit. Dynamic heat inputs are not directly measurable and difficult to estimate, but need to be compensated.

3.3 Modelling

q_{1c} and q_{1h} in Eq. (3) and Eq. (5) can be written following empirical newtonian law as function of global heat transfer coefficient, exchange surface and temperature difference, both reported to the cold and hot surface. Based on this equations, the state space representation for the condenser model is given below in Eq. (6), where $\dot{m}_{l,N_2}$ is liquid nitrogen mass flow and the input to the system, and x_{vap} the percentage of liquid nitrogen evaporating inside the heat exchanger tube. We assume nitrogen quality at the input is close to 0%.

$$\begin{bmatrix} \dot{T}_{Kr} \\ \\ \dot{T}_{Ar} \end{bmatrix} = \begin{bmatrix} \dfrac{q_s + q_d}{k_2 \cdot h_{lg,Kr}} - \dfrac{q_{1h}}{k_2 \cdot h_{lg,Kr}} \\ \\ \dfrac{q_{1c}}{k_1 \cdot h_{lg,Ar}} - \dfrac{x_{vap} \cdot \dot{m}_{l,N_2} \cdot h_{\mathrm{lg},N_2}}{k_1 \cdot h_{lg,Ar}} \end{bmatrix} \tag{6}$$

The differential equations can be expressed under the following model of representation, described in Eq (7).

$$\dot{X} = A \cdot X + B \cdot U + \mathrm{w} \tag{7}$$

Where X is the state vector, $[T_{Kr}, T_{Ar}]$, U is the command vector and w contains the *a priori* unknown dynamics. This representation has the advantage to take into account the imperfection of the *a priori* known modelling part. A and B are two matrix which provides a commendable result. A and B are respectively describes in Eq (8) and 9.

$$A = \begin{bmatrix} -\dfrac{H_{1h} \cdot S_{1h}}{k_2 \cdot h_{\mathrm{lg},Kr}} & \dfrac{H_{1h} \cdot S_{1h}}{k_2 \cdot h_{\mathrm{lg},Kr}} \\ \\ \dfrac{H_{1c} \cdot S_{1c}}{k_1 \cdot h_{\mathrm{lg},Ar}} & -\dfrac{H_{1c} \cdot S_{1c}}{k_1 \cdot h_{\mathrm{lg},Ar}} \end{bmatrix} \tag{8}$$

$$B = \begin{bmatrix} 0 & -\dfrac{x_{vap} \cdot h_{\mathrm{lg},N_2}}{k_1 \cdot h_{\mathrm{lg},Ar}} \end{bmatrix}^T \tag{9}$$

Analysing matrix A, one of the eigenvalues is equal to zero providing an instability of the system. By numerical application, we notice the system is commendable for approximative values of A and B.

3.4 Time Delay Control approach

Time Delay Control has been developed 20 years ago for systems described by differential equations including unknown terms. Proposed by Youcef-Toumi and Ito [12], it was applied on nonlinear systems under two main conditions, all state variables must be measurable and a continuous signal conserve a quite constant value on a sufficiently small time period. This terms are estimated from past commands and state variables information. The estimator principle of the unknown term is defined in Eq. (10) as the output of a delay operator D.

$$\hat{\mathrm{w}}(t) = D \cdot \left(\dot{X}(t) - AX(t) - BU(t) \right) \tag{10}$$

The corresponding Laplace transform of time delay is e^{-Ls}, which can be estimate by Padé approximant. According to our model, we define a second order Padé approximation, developed in Eq. (11). the resulting transfer function has to be stable, causal and with a unitary static gain.

$$G_{m/n}(s) = \frac{d_0 + p_1 s}{d_0 + d_1 s + d^2 s^2} \tag{11}$$

In parallel, we arbitrary choose a reference linear model implying the trajectory to follow, where matrix A_r and B_r are constant, A_r is stable and the couple (A_r, B_r) is commendable. The command signal is developed in Eq. (12) where B^+ is matrix B pseudo inverse, c is the set point vector.

$$u = B^+ \left[B_r c + (A_r - A) X - \hat{\mathrm{w}} \right] \tag{12}$$

$\hat{\mathrm{w}}$ in Eq. (12) can be substituted by the Laplace transform of its expression in Eq. (10) with Padé approximant. As shown in Fig. (3), the controller model uses state variables, consequently, they have to be available, physically or by a state rebuilder.

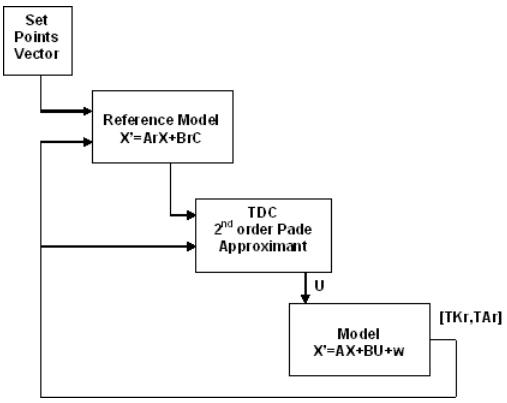

Fig. 3 Simulated Model with Time Delay Control

3.5 Discussion

Fig. (4) shows stability differences between classical PI controller tuned as in cryogenics process (characterized by a large integration time, which is a compromise between set point tracking, inverted response and dynamics compensation) and a Time Delay controller. After

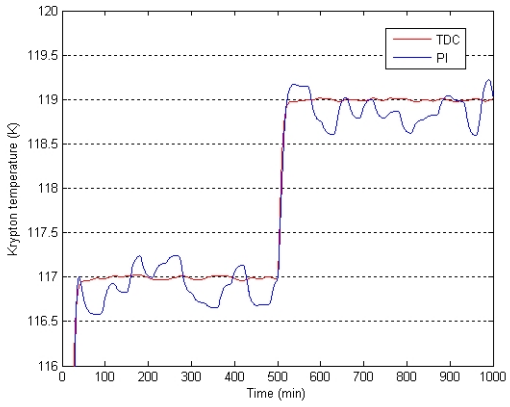

Fig. 4 Comparison between PI controller and TDC with set point variation for small dynamics.

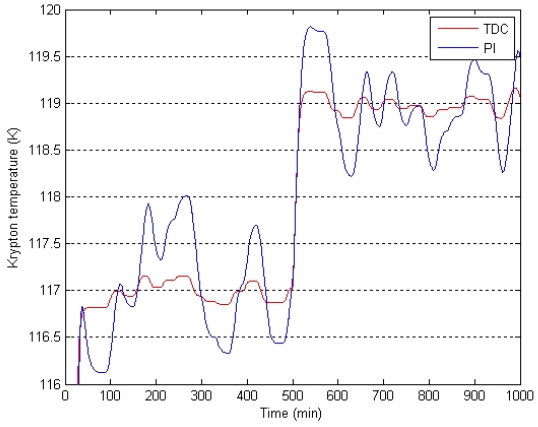

Fig. 5 Comparison between PI controller and TDC with set point variation for enlarged dynamics.

approximated numerical applications, both responses are based on the same model, included random parameters to represent the static and dynamic heat inputs in liquid krypton. Fig. (5) present a simulation with exaggerated dynamics to face the reactivity of Time Delay Control. In both cases, it occurs that TDC has a better efficiency on krypton temperature regulation and keep T_{Kr} variations between $\pm 0.1\ K$. Krypton temperature set point is varying between $117\ K$ and $119\ K$. Saturated pressure can easily be reported to saturated temperature. Between $116.5\ K$ and $118\ K$, saturated pressure difference is close to $100\ mbar$.

The estimation of w from first order and second order Padé approximants, on Fig. (6), gives satisfying results. The approximation by first order transfer function is closer to the unknown dynamics but do not improve significantly the state variables stability. In both cases, the static part of w is clearly identified and the dynamic is well followed.

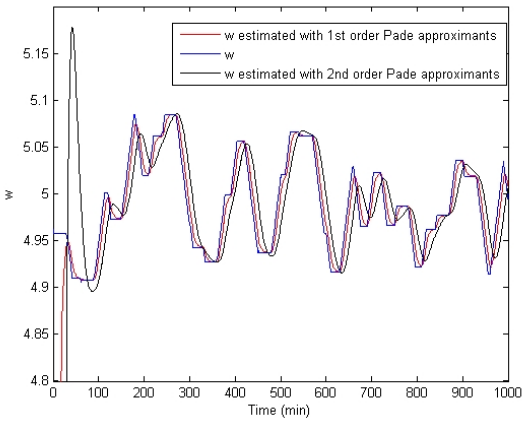

Fig. 6 Estimation of unknown parameters linked to dynamic heat inputs.

4 Extended nonlinear model

Forced convection vaporization is an important mode of heat transfer that occurs in applications such as cryogenics and refrigeration (Air-Conditioning system for example), power generation and process industries. The cooling energy used is related to the nitrogen latent heat of vaporization and to the quantity of vaporized mass. A nonlinear observer design for two-phase flow heat exchanger has been done by Cheng, He and Asada [13] using only differential equations. The difficulty is to modelize the nonlinear behavior and to measure vapor quality and wet area.

The correlation of vapor quality at the outlet and wet area aims to complete the first model in determining the quantity of liquid nitrogen we need, to reach steady state through a better control of the liquid nitrogen mass flow, integrating pressure control. There is no feedback circuit to get back the liquid nitrogen, therefore the vapor quality at the outlet has to be properly controlled to a high rate (close to 90%) in case we need all the length of the tube. Accordingly, the number of state variables increases. Based on several surveys already mentionned previously, we propose to add liquid nitrogen heat exchanger wall tempearature,T_{wall} , length of wet area and mean void fraction along the two phase section. The new model can be divided into two parts, depending on l, which is the length of the two phase section. It is assumed that the two phase section has invariant mean void fraction $\bar{\alpha}$ if $l < L$, with L the total length of the nitrogen heat exchanger tube. First, the expression of q_2 in Eq. (3) must be replaced by Eq. (13) where R_e and h_e has been defined previously.

$$q_2 = 2\pi R_e \cdot l \cdot h_e \cdot (T_{Ar} - T_{wall}) \qquad (13)$$

T_{wall} derivative can be expressed from its energy balance equation, considering its specific heat, c_p, and heat transfer with nitrogen from one part, and with argon from the other part. The liquid mass balance equation in the two phase section of the evaporator has two expression depending on the rate of liquid nitrogen evap-

orating into vapor.

$$\begin{cases} \rho_{l,N_2}\left(1-\bar{\alpha}\right)A\dfrac{dl\left(t\right)}{dt}=\dot{m}_{in}-\dfrac{q_3}{h_{lg,N_2}} & \text{if} l(t)<L \\ \rho_{l,N_2}\cdot L A\dfrac{d\left(1-\bar{\alpha}\right)\left(t\right)}{dt}=\dot{m}_{in}-\dfrac{q_3}{h_{lg,N_2}} & \text{if} l(t)\geq L \end{cases} \quad (14)$$

Eq. (14) describes the derivative we need to consider in a function of $l\left(t\right)$. $\bar{\alpha}$ is the mean void fraction, it can be related to x_{out}, the outlet vapor quality, in case $x_{out} < 1$. To alleviate the writing of $(1-\bar{\alpha})$, we will represent it by $\bar{\alpha}^*$. ρ_{l,N_2} represents liquid nitrogen density, and A the cross section area of the heat exchanger tube.

Therefore, the new state vector is written in Eq. (15), where $l\left(t\right)$ and $\bar{\alpha}^*\left(t\right)$ are continuous but limited functions, $0 \leq \bar{\alpha}^*\left(t\right) \leq 1$ and $0 \leq l\left(t\right) \leq L$.

$$X\left(t\right)=\left[T_{Kr}(t)\,,T_{Ar}(t)\,,T_{wall}(t)\,,l(t)\,,\bar{\alpha}^*(t)\right]^T \quad (15)$$

It occurs a nonlinear model, especially from the bilinear function of l and $(T_{wall}-T_{N_2})$ in the expression of q_3. Moreover, part of the state is not measurable. In using outlet valve, saturated nitrogen pressure is modified, it directly means the saturated nitrogen temperature T_{N_2}. Command vector contains two variables, instead of one previously. The extended model can be expressed under the following configuration, as shown in Eq. (16).

$$\dot{X} = f\left(X\right) + B\left(X\right)U + \mathrm{w}\left(t\right) \quad (16)$$

Several variant have been proposed for Time Delay Control, especially for nonlinear systems with this kind of representation. Idea can be to use first a state rebuilder to have the complete state vector. Fig. (7) presents a possible control approach based on a nonlinear model.

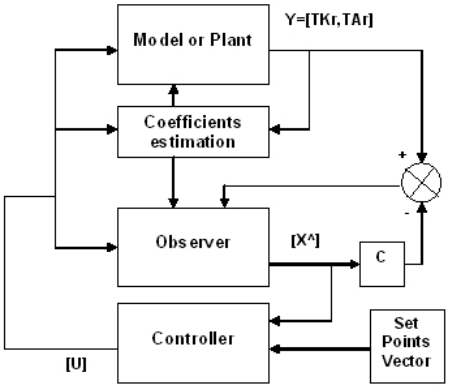

Fig. 7 Extended Model Observation and Control Approach.

5 Integration

In order to use the previous work in the global cryogenic control system, we had to find a solution to integrate the model without disordering the process logic in the new Siemens PLC. Assuming the fact that we need to modify and tune the model parameters estimation several times, and probably to disconnect it from the PLC, the Modelling Workstation is in a separate unit, exchanging data through OPC© (OLE for Process Control). Simatic Net gives the opportunity to include an OPC server function which communicates with the S7 CPU to send measurements to the modelling station. A global scheme is shown in Fig. (8), but it is not currently processing and connected to the real plant due to the actual S5-PLC installation and the risks in modifying such an installation which is running. The modelling workstation is connected on the ethernet network, communicating with the S7-PLC on an OPC layer. the OPC server is embedded in the MWS and OPC toolbox of the simulation software extracts data, as an interface, to compare measurements with model outputs. Several coefficients are not constant and need to be redetermined from data sent by the S7-PLC. Thanks to tables, determined with ALLPROPS Software, and interpolation functions, the model coefficients can be approximate with an arbitrary resolution, depending on tables dimensions. Dedicated variables in the S7 PLC receives model outputs and are available in the *Operating WorkStation* to compare the results directly on the cryogenics control HMI.

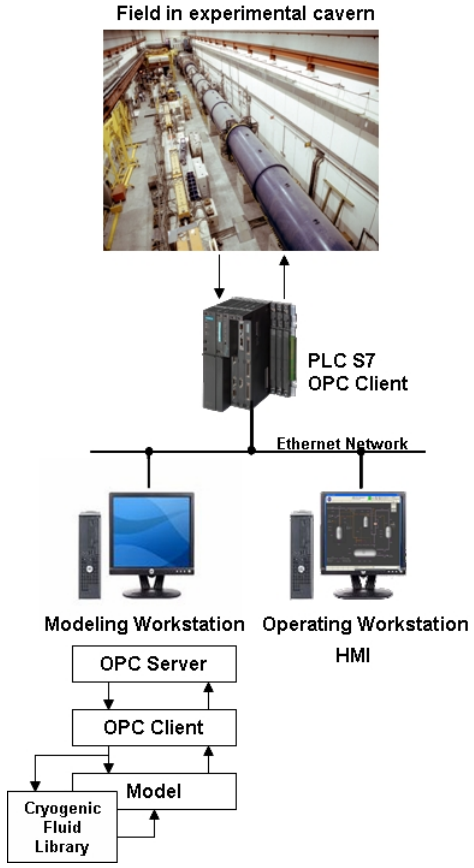

Fig. 8 Model integration in CERN Control Architecture.

6 Conclusion and Perspectives

Modelling step developed a better overview and knowledge of the cryogenics process and on its nonlinearities. We are conscious that several assumptions have been done but the results, in working with Time Delay Control, were able to compensate a part of the approximations. In the next months, the modelling workstation will be in progress and will probably start its tuning period on a cryogenic test bench with argon and nitrogen, to confirm the results of the simulations and to improve its precision.

7 Acknowledgments

The authors would like to thank cryogenic engineers from ECR (Cryogenics for Experiments) group at CERN and Claudia Cogne from the Picardie Jules Verne University for the help they gave to check the models equations.

8 References

[1] Johan Bremer and al. "the liquid krypton calorimeter cryogenics for the na48 experiment". *International Cryogenic Engineering Conference*, 17:892–904, 1998.

[2] Steven G. Penoncello Richard T Jacobsen and Eric W. Lemmon. *"Thermodynamics Properties of Cryogenic Fluids"*. Plenum Press, New York, 1997.

[3] L. Doretti G.A. Longo A. Cavallini, D. Del Col and L. Rosetto. "a new computational procedure for heat transfer and pressure drop durin refrigerant condensation inside enhanced tubes". *Journal of Enhanced Heat Transfer*, 6:441–447, 1999.

[4] S.G. Kandlikar and T. Raykoff. "predicting flow boiling heat transfer of refrigerants in microfin tubes". *Journal of Enhanced Heat Transfer*, 4:257–268, 1997.

[5] Y.Y. Hsu. "a review of film boiling at cryogenic temperatures". *Advances in Cryogenic Engineering*, 17:361–381, 1972.

[6] Randall F. Barron. *"Cryogenic Heat Transfer"*. Taylor & Francis, Philadelphia, 1999.

[7] N. Özisik. *"Heat transfer: a basic approach"*. McGraw-Hill, 1985.

[8] J.F. Sacadura. *"Initiation aux transferts thermiques"*. Tech et Doc, 1993.

[9] A.C. Cleland S. Estrada-Flores, D.J. Cleland and R.W.James. "simulation of transient behaviour in refrigeration plant pressure vessels: mathematical models and experimental validation". *International Journal of Refrigeration*, 26:170–179, 2003.

[10] S. Skogestad E. Stoorkas and J.M. Godhavn. "a low-dimensional dynamic model of severe slugging for control design and analysis". *Multiphase'03, San Remo, Italy*, 2003.

[11] Gerhard Nygaard and Geir Naevdal. "modelling two-phase flow for control design in oil well drilling". *IEEE Conference on Control Applications*, pages 675–680, 2005.

[12] K. Youcef-Toumi and O Ito. "controller design for systems with unknown dynamics". *Proceeding of American Control Conference*, 1987.

[13] Xiang-Dong He Tao Cheng and Harry Asada. "nonlinear observer design for two-phase flow heat exchangers of air conditioning systems". *ASME*, 2004.

